



# One-step synthesis of a Methylene Blue@ZIF-8-reduced graphene oxide nanocomposite and its application to electrochemical sensing of rutin

Zonghua Wang<sup>1</sup> · Gege Yu<sup>1</sup> · Jianfei Xia<sup>1</sup> · Feifei Zhang<sup>1</sup> · Qingyun Liu<sup>2</sup>

Received: 13 November 2017 / Accepted: 12 April 2018 / Published online: 3 May 2018  
© Springer-Verlag GmbH Austria, part of Springer Nature 2018

## Abstract

The authors demonstrate the exploitation of reduced graphene oxide (RGO) as a template for immobilizing zeolitic imidazolate framework-8 (ZIF-8) crystals loaded with the electrochemical probe Methylene Blue (MB). The framework was deposited on the surface of RGO in a one-pot process. Transmission electron microscopy, scanning electron microscopy and X-ray diffraction were employed to characterize the nanocomposite. The electrochemical behavior of rutin at a glassy carbon electrode (GCE) modified with the nanocomposite was investigated by cyclic voltammetry and differential pulse voltammetry. The modified GCE displays high electrocatalytic activity toward rutin oxidation at a relatively low working potential (0.4 V vs. Ag/AgCl). Under the optimal conditions, the sensor has an amperometric response that is linear in the 0.1 to 100  $\mu\text{M}$  rutin concentration range, with a 20 nM detection limit (at an S/N ratio of 3). The method was successfully applied to the determination of rutin in tablets and urine samples.

**Keywords** Electrochemistry · Sensor · Nanocomposite · Electroanalysis · Cyclic voltammetry · Differential pulse voltammetry · Electrocatalytic activity · Amperometric response

## Introduction

Rutin (3',4',5,7-tetrahydroxyflavone 3 $\beta$ -D-rutinoside) is a kind of commonly found flavonoid glycosides, which is also called vitamin P. Rutin has anti-inflammatory, anti-bacterial, anti-tumoral and anti-oxidative properties. It has been widely used as a therapeutic medicine, which can lower blood pressure, reduce capillary permeability and dilute the blood [1]. Therefore, the rapid, accurate and sensitive determination of rutin is

important in clinical and pharmaceutical analysis. Up to date, some analytical methods have been established for this purpose, including high-performance liquid chromatography (HPLC) [2], UV-vis spectrophotometry [3], reversed-phase liquid chromatography (RPLC) [4], flow injection analysis (FIA) [5], sequential injection analysis [6] and electrochemical methods [7]. Among these methods, the electroanalytical method exhibits many advantages, such as convenient procedure, low cost, short analysis time and high sensitivity. For example, Zhou et al. have prepared a modified electrode by using multi-walled carbon nanotubes and gold nanoparticle as the modifier and investigated the electrochemical behavior of rutin on this electrode by cyclic voltammetry [8]. Wu et al. have prepared a Fe<sub>2</sub>O<sub>3</sub>/RGO hybrid film modified electrode and applied the electrode to amperometric sensing of rutin [9]. In spite of several modified electrodes have been reported for detection of rutin, it is also important to fabricate new modified electrode with great performances for rutin.

Metal-organic frameworks (MOFs) consist of inorganic metal ions and organic linker molecules. Owing to their large surface areas, high porosity, ordered crystalline structures, excellent mechanical stability and structural tunability (pore sizes, pore shape, surface area) [10], MOFs have been applied in various field including gas storage and separation [11], catalysis

**Electronic supplementary material** The online version of this article (<https://doi.org/10.1007/s00604-018-2796-4>) contains supplementary material, which is available to authorized users.

✉ Jianfei Xia  
xijianfei@126.com

<sup>1</sup> College of Chemistry and Chemical Engineering, Shandong Sino-Japanese Center for Collaborative Research of Carbon Nanomaterials, Collaborative Innovation Center for Marine Biomass Fiber Materials and Textiles, Laboratory of Fiber Materials and Modern Textile, the Growing Base for State Key Laboratory, Qingdao University, Qingdao 266071, People's Republic of China

<sup>2</sup> College of Chemistry and Environmental Engineering, Shandong University of Science and Technology, Qingdao, People's Republic of China

[12], energy storage [13] and chemical sensing [14]. Therefore, there have been increasing concerns about the application of MOFs in the electrochemical field [15, 16]. Zeolitic imidazolate frameworks (ZIFs) is an attractive subclass of MOFs due to the ease of synthesis, the great thermal, hydrothermal and chemical stabilities [17]. Among the ZIFs, ZIF-8 have attracted much interest, which is a kind of ZIFs built from zinc ions and 2-methylimidazolate. However, most of the MOFs are insulators and the direct application of single MOFs in electrochemistry is limited by their poor conductivity and weak electrocatalytic abilities [18]. In order to solve this problem, it was proposed to introduce the highly electroconductive and electroactive materials into MOFs. Among the electroconductive materials, graphene has received extensive attention for electrochemical analysis owing to its extraordinary electrical conductivity, exceptional electron transfer rate and high mechanical strength [19–21]. For example, Yu et al. have prepared a novel MOFs/graphene nanocomposite through the in-situ synthesis method and used as a novel electrochemical sensor for ultrasensitive detection of dopamine [15]. The fabricated electrode showed great potential applications in the detection of DA with remarkable enhanced effect on voltammetric response of DA. Wang et al. have prepared Cu(tpa)-GO nanocomposites for the determination of acetaminophen (ACOP) and dopamine(DA) [22]. Due to the synergistic effect of graphene and Cu(tpa) crystals, the composites possessed the higher accessible surface area and conductivity, which improved the electrochemical detection sensitivity. In order to further improve the electrochemical performances of the MOFs/graphene nanocomposite, the introduction of another component with electroconductivity and electroactivity may be an effective strategy.

In this work, the cationic dye methylene blue (MB), which is an electron transfer mediator, was loaded in ZIF-8 crystals as another component for MOFs/graphene nanocomposite. Incorporation of dye MB molecules inside the ZIF-8 matrix can protect the dye from affecting by the surrounding environment and enhance the

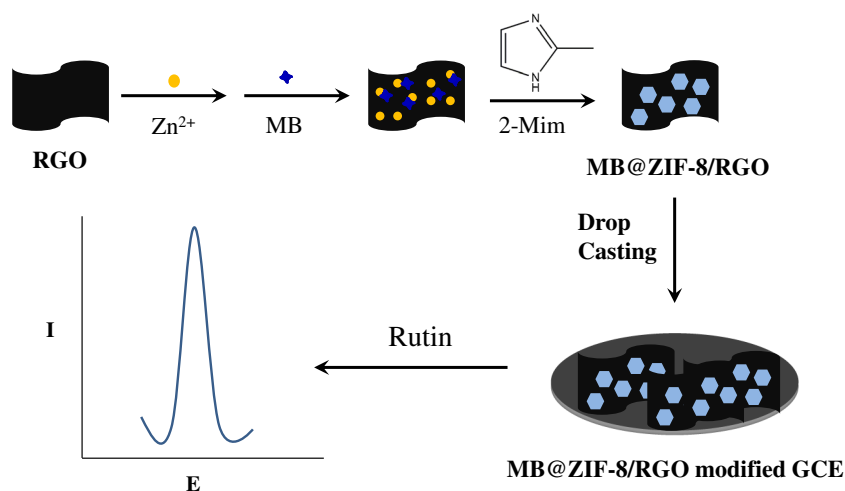
electroconductivity and electroactivity of the MOFs material. And the MB loaded ZIF-8 (MB@ZIF-8) was decorated on the surface of reduced graphene oxide (RGO) in one-pot process by using RGO as template for immobilizing MB@ZIF-8. The MB@ZIF-8/RGO nano hybrid was deposited on the surface of a glassy carbon electrode (GCE) to construct electrochemical sensor for rutin. The high surface area, electroconductivity and electroactivity of the MB@ZIF-8/RGO nano hybrid allowed the efficient oxidation of rutin. And the MB@ZIF-8/RGO nano hybrid modified electrode exhibited low detection limit, high sensitivity and a wide linear range for electrochemical detection of rutin. The schematic diagram for the fabrication of the modified electrode and the detection of rutin is shown in Scheme 1. This method was applied to the detection of tablet samples, and the results were satisfactory.

## Experimental

### Reagents

Graphite was provided by Qingdao Fujin Graphite Co., Ltd. (Qingdao, China).  $\text{Zn}(\text{NO}_3)_2 \cdot 6\text{H}_2\text{O}$  and 2-methylimidazole (2-MIM) were obtained from Aladdin Reagent Co., Ltd. (Shanghai, China. [www.aladdin-e.com/](http://www.aladdin-e.com/)). Methylene blue were obtained from Shanghai Reagent Factory (Shanghai China). Rutin and quercetin were obtained from Sigma-Aldrich (St. Louis, MO, USA). HCl, NaOH and ethanol were obtained from Tianjin Regent Co., Ltd. (Tianjin, China). Phosphate buffer with different pH values (from 6.0 to 8.0) were prepared by mixing 0.02 M NaCl,  $\text{NaH}_2\text{PO}_4 \cdot 2\text{H}_2\text{O}$  and  $\text{Na}_2\text{HPO}_4 \cdot 12\text{H}_2\text{O}$  and adjusting the pH with HCl or NaOH. All chemicals were of analytical grade and used without further purification. Doubly distilled water (DDW) was used throughout the experiments, and the experiments were performed at room temperature.

**Scheme 1** Schematic diagram for the fabrication of the modified electrode and the detection of rutin



## Apparatus

Transmission electron microscope (TEM) images were obtained by JEOL JEM-2100 (Japan). Scanning electron microscopy (SEM) images were obtained by JEOL JSM-7001F (Japan). X-ray diffraction (XRD) was operated on a Rigaku Ultima IV diffractometer (Japan). Cyclic voltammetry (CV) and differential pulse voltammetry (DPV) were performed on CHI-660C electrochemical workstation (Shanghai Chenhua Instrument Co., Ltd., China) with a conventional three-electrode system: an Ag/AgCl electrode (Ag/AgCl) was used as the reference electrode, a platinum wire was used as the auxiliary electrode, and the bare or modified glassy carbon electrode was used as the working electrode.

## Preparation of ZIF-8, MB@ZIF-8 and MB@ZIF-8/RGO nanocomposites

ZIF-8 was synthesized in an aqueous system according to the previous literature [15]. The synthesis of ZIF-8 crystals loading methylene blue (MB@ZIF-8) was performed in previous way [23]. GO was synthesized from graphite powder by employing a modified Hummers' method, and RGO was prepared by reducing the synthesized GO with hydrazine [19]. MB@ZIF-8/RGO nanocomposites were synthesized by the RGO-templated growth of ZIF-8 loaded methylene blue in a one-pot process [24]. The detailed synthesis procedures were shown in Electronic Supporting Material.

## Preparation of MB@ZIF-8/RGO modified electrode

Prior to modification, the bare GCE was sequentially polished with 0.3  $\mu\text{m}$  and 0.05  $\mu\text{m}$  alumina slurry on a polishing cloth. Then the GCE was rinsed ultrasonically in ethanol and DDW for 2 mins and dried by  $\text{N}_2$  for further use. 2 mg prepared MB@ZIF-8/RGO was ultrasonic dispersed in 2 mL of DDW to obtain the 1.0 mg  $\text{mL}^{-1}$  homogeneous dispersion. Then 6  $\mu\text{L}$  of RGO/ZIF-8 dispersion was dropped on the electrode surface and dried under the room temperature to obtain the MB@ZIF-8/RGO modified GCE (MB@ZIF-8/RGO/GCE). For comparison, the ZIF-8 modified GCE (ZIF-8/GCE), RGO modified GCE (RGO/GCE) and MB@ZIF-8 modified GCE (MB@ZIF-8/GCE) were prepared only by replacing the MB@ZIF-8/RGO dispersion with ZIF-8, RGO or MB@ZIF-8 solutions.

## Electrochemical measurement

0.10 M phosphate buffer was employed as the supporting electrolyte. All electrochemical experiments were implemented at room temperature by using an electrochemical cell (10 mL) with a standard three-electrode system. The bare or modified glassy carbon electrode was used as the

working electrode. Electrochemical studies on the determination of rutin were performed by using CV and DPV in phosphate buffer (pH 7.0) with following parameters: pulse amplitude of 50 mV, increment potential of 4 mV, pulse width of 0.2 s and pulse period of 0.5 s. The potential ranges were from  $-0.4$  to 1.0 V, and the scanning rate was  $100 \text{ mV}\cdot\text{s}^{-1}$ .

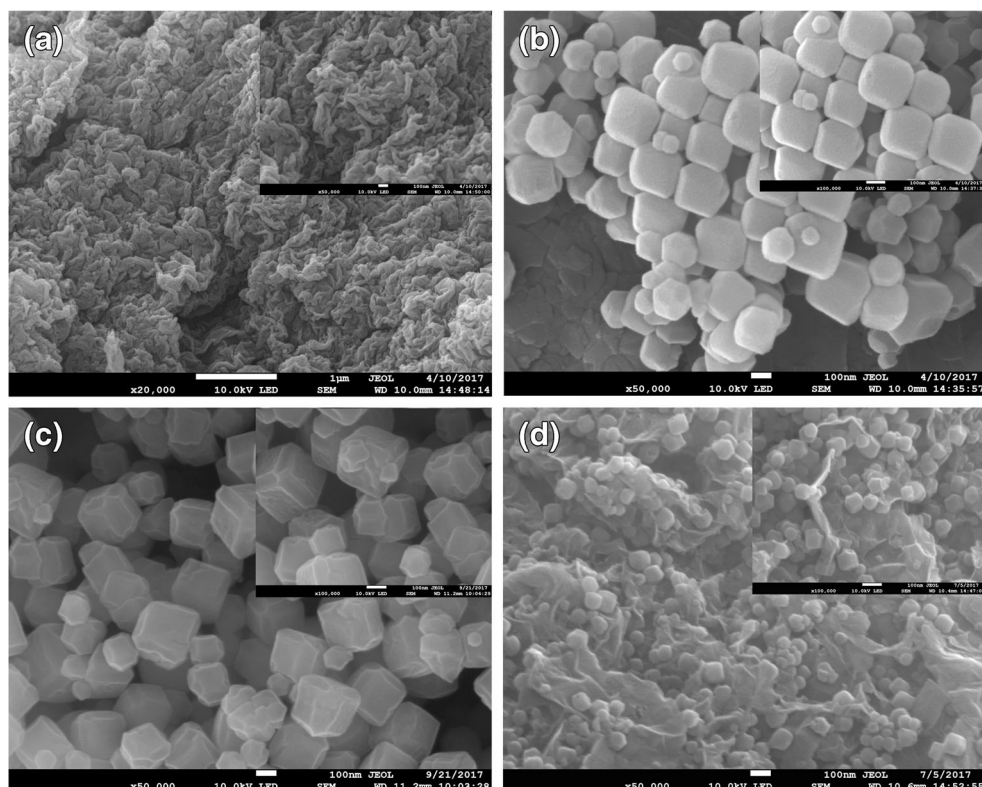
## Results and discussion

### Characterization of ZIF-8, RGO, MB@ZIF-8 and MB@ZIF-8/RGO

Figure 1 displays the SEM images of the synthesized RGO, ZIF-8, MB@ZIF-8 and MB@ZIF-8/RGO. As can be seen from the image of RGO (Fig. 1a), a large amount of thin and crumpled sheets form a disordered structure containing crack-shaped large pores. The SEM images of ZIF-8 (Fig. 1b) exhibit hexagonal morphology ZIF-8 nanoparticles and reveal that ZIF-8 consists of isolated distributed nanoparticles with diameter 100–300 nm. From Fig. 1c, we observe that MB@ZIF-8 shows isolated particles distribution and hexagonal morphology in accordance with the ZIF-8 nanoparticles. From the SEM image of MB@ZIF-8/RGO nanocomposite (Fig. 1d), it can be seen that isolated MB@ZIF-8 particles with diameter 70–100 nm are anchored on both internal and external surfaces of RGO. RGO are not only coated on the surface of MB@ZIF-8 particles but also interconnected isolated MB@ZIF-8 crystals. The TEM analysis has the similar results (in the Electronic Supplementary Material).

The XRD analysis of GO, RGO, ZIF-8, MB@ZIF-8 and MB@ZIF-8/RGO are shown in Fig. 2a. The GO sheets reveal a strong peak at  $2\theta = 11.3^\circ$ , corresponding to the (001) reflection. A broad peak with  $2\theta$  values of  $23.5^\circ$  (002) is the characteristic diffraction peak of RGO, which is resulted from the reduction of GO. The obvious changes indicate that RGO is successfully obtained from GO. All diffraction peaks of ZIF-8 can be attributed to typical crystal structure of ZIF-8, indicating successful synthesis of pure-phase ZIF-8 material [25]. The diffraction patterns of MB@ZIF-8 and MB@ZIF-8/RGO particles are consistent with that of ZIF-8, which demonstrates that the presence of MB and RGO sheets did not break the formation of the ZIF-8 crystal structure. Compared with ZIF-8, the peak intensity at the low angles decreases for MB@ZIF-8, which is due to the presence of MB molecules in the pores of ZIF-8 crystals [23]. What is more, the ZIF-8 particles are white particles and the color of MB@ZIF-8 becomes blue (Fig. 2b), which indicates that the MB molecules have been successfully loaded into the ZIF-8 crystals.

**Fig. 1** SEM images of RGO (a), ZIF-8 (b), MB@ZIF-8 (c) and MB@ZIF-8/RGO (d)

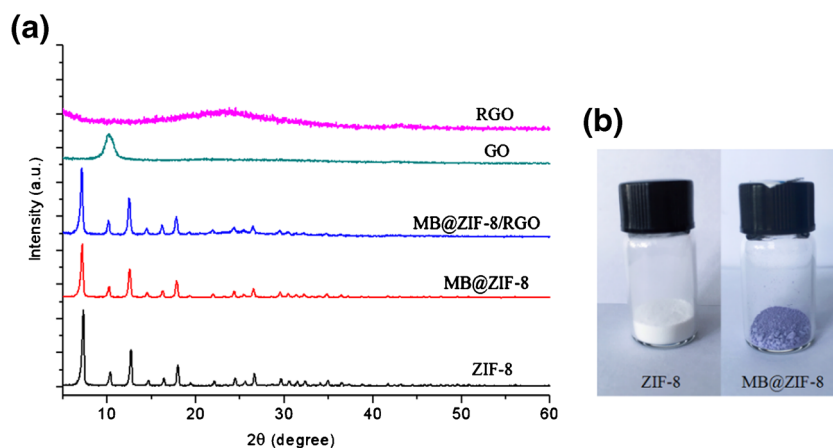


### Electrochemical behaviors of modified electrodes

CV of the ferricyanide system is a useful tool to characterize the electrochemical behaviors of the electroactive species on the modified electrode surface. Figure 3 shows a comparison of the electroactivity among different modified electrodes investigated by CV in 0.1 M KCl solution containing 5 mM  $K_3Fe(CN)_6$ . For bare GCE (curve a), a couple of well-defined redox peaks are observed with peak-to-peak separation ( $\Delta E_p$ ) of 145 mV. For ZIF-8/GCE (curve b), though the ZIF-8 has high specific surface area and

porosity, the peak currents of redox peaks have no obvious changes and the  $\Delta E_p$  value increases, which is due to the poor conductivity and slow electron transfer of ZIF-8 nanoparticle. When the electrode is coated with MB@ZIF-8 (curve c) and RGO/ZIF-8, (curve d), the peak currents of redox peaks increase obviously. When the electrode is coated with MB@ZIF-8/RGO (curve e), the redox peak currents increase significantly and the  $\Delta E_p$  value decreases to 96 mV, which can be attributed to the synergistic effects from highly electrical conductivity of RGO, high electroactivity of MB and porosity of ZIF-8.

**Fig. 2** XRD patterns of RGO, GO, ZIF-8, MB@ZIF-8 and MB@ZIF-8/RGO (a); and photographs of ZIF-8 and MB@ZIF-8 particles (b)



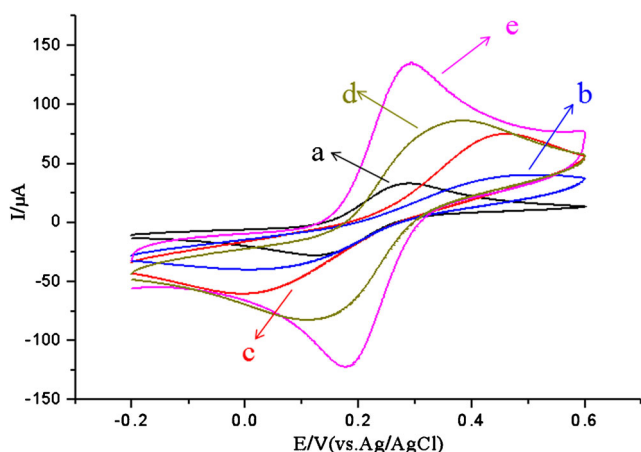


**Fig. 3** CV curves of bare GCE (a), ZIF-8/GCE (b), MB@ZIF-8/GCE (c), RGO/ZIF-8/GCE (d) and MB@ZIF-8/RGO(e) in 0.1 M KCl solution containing 5 mM  $K_3Fe(CN)_6$ . Scan rate = 100  $mV s^{-1}$

### Electrochemical parameters of rutin at RGO/ZIF-8/GCE

The influence of supporting electrolyte pH on the peak potentials ( $E_p$ ) and peak currents ( $I$ ) of the electrochemical detection of rutin at MB@ZIF-8/RGO/GCE was investigated by CVs in a pH range of 6.0–8.0. In Fig. S2 (in Electronic Supporting Material), the maximum of redox current emerges at the pH 7.0, which is chosen as the optimal working pH in the following investigation for sensitivities. From the inset, it is clear that the oxidation peak potentials of the rutin shift to negative values with the increase of pH. The linear regression equation of the oxidation peak can be expressed as  $E_{pa}$  (V) = 0.739–0.0614 pH,  $R^2 = 0.996$ . The slope value of 61.4  $mV \cdot pH^{-1}$  is close to the theoretical value of 59  $mV \cdot pH^{-1}$ , indicating that the same amounts of electrons and protons take

part in the electrode reaction. The redox mechanism of rutin at the MB@ZIF-8/RGO/GCE is illustrated in Fig. 4, and it can be seen that two electrons and two protons are involved in the reaction [9].

The effect of scan rate on the electrocatalytic activity was also observed by CV tests in phosphate buffer (pH 7.0) containing 0.10 mM rutin (Fig. S3 in Electronic Supporting Material). As the scan rate increasing from 10 to 600  $mV \cdot s^{-1}$ , the redox peak currents increase gradually. A good linear relationship between the peak current ( $I_p$ ) and the scan rate ( $v$ ) is plotted (Inset of Fig. S2) with the linear regression equation as  $i_{pa}$  ( $\mu A$ ) = 2.3538 + 0.1376  $v$  ( $mV \cdot s^{-1}$ ) ( $R^2 = 0.999$ ) and  $i_{pc}$  ( $\mu A$ ) = –9.3364–0.1011 $v$  ( $mV \cdot s^{-1}$ ) ( $R^2 = 0.999$ ), respectively, suggesting that the electrode reaction of rutin is a predominantly adsorption-controlled process. Moreover, with the increase of scan rate, the anodic peak potential shifts toward a more positive value and the cathodic peak potential shifts toward a more negative value, and the peak-to-peak separation ( $\Delta E_p$ ) increases. According to Laviron's equation [26], the electron transfer number ( $n$ ) was calculated to be two. So, there are two electrons involved in the electrode reaction which was in agreement with the previous works [27].

### Determination of rutin

The loading amount of MB@ZIF-8/RGO has a profound influence on the electrochemical response. In order to study the optimal loading of modifier on GCE, a series of modified electrodes are fabricated with different amounts of MB@ZIF-8/RGO and their electrochemical responses to rutin are investigated by DPV (Fig. S4 in Electronic Supporting Material). The

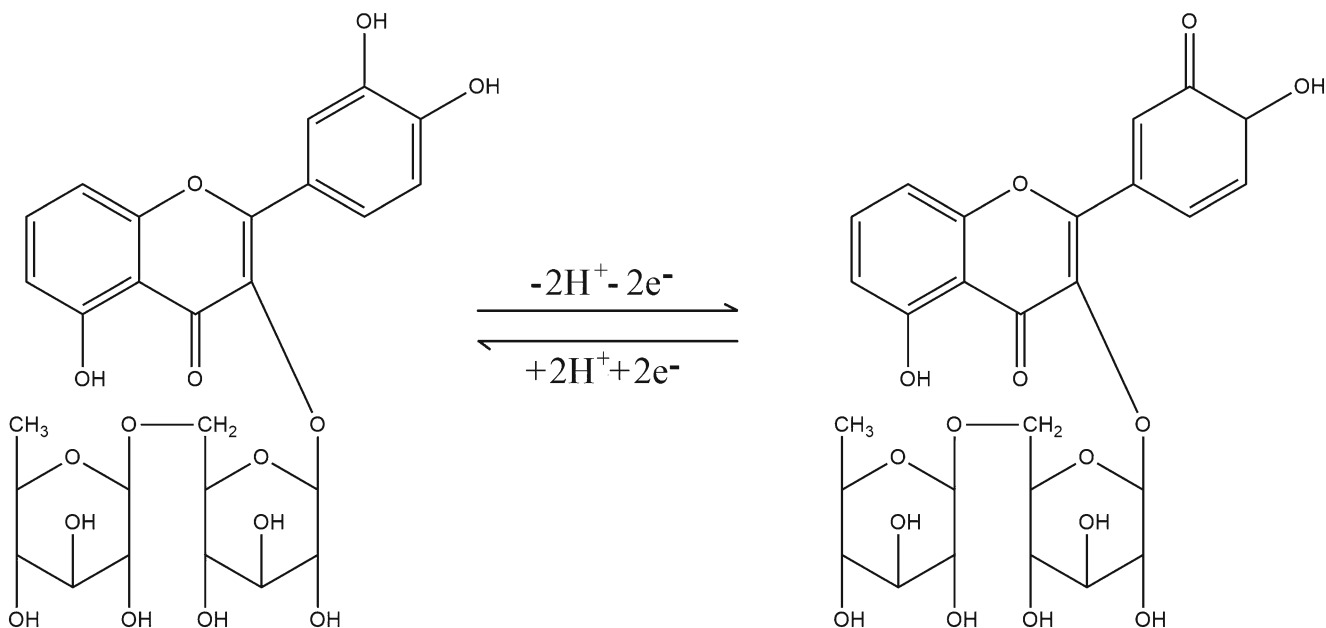
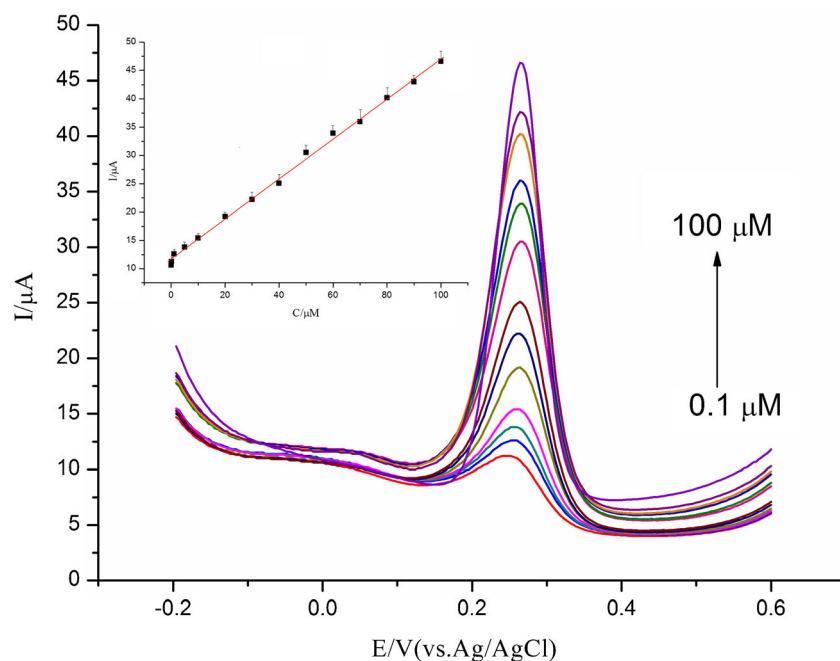


**Fig. 4** Electrochemical reaction mechanism of rutin

**Fig. 5** DPV curves for different concentrations of rutin (from bottom to top: 0.1, 1, 5, 10, 20, 30, 40, 50, 60, 70, 80, 90, 100  $\mu\text{M}$ ) at the MB@ZIF-8/RGO/GCE in 0.1 M phosphate buffer of pH 7.0 (scan rate: 100 mV s<sup>-1</sup>). Inset: The linear calibration plots of the peak currents ( $I_p$ ) versus rutin concentrations



anodic peak currents increase rapidly upon increasing the loading amount of modifier from 2 to 6  $\mu\text{L}$ . However, the anodic peak currents tend to decrease from 6 to 10  $\mu\text{L}$ , which results in a decreased electrochemical response. Therefore, the 6  $\mu\text{L}$  amount of modifier is chosen for subsequent studies.

Under the optimal conditions, DPV was used to determine the rutin with different concentrations at the MB@ZIF-8/RGO/GCE (Fig. 5). In the inset of Fig. 5, the oxidation peak current of rutin ( $I_p$ ,  $\mu\text{A}$ ) is linear with its concentrations ( $C$ ,  $\mu\text{M}$ ) in the range of 0.1  $\mu\text{M}$  to 100  $\mu\text{M}$ . The relationships can be described as follows:  $i_p$  ( $\mu\text{A}$ ) = 12.1566 + 0.3446  $c$  ( $\mu\text{M}$ ) with a linear correlation coefficient of 0.997. Based on the signal-to-noise ratio of 3 ( $S/N=3$ ), the detection limit is calculated to be 20 nM. Table 1 summarizes the comparison of the analytical

performances of the MB@ZIF-8/RGO/GCE with other reported electrochemical methods for rutin determination. As well seen, the fabricated modified electrode shows a reasonable linear range and the detection limit was lower than or equal to most of the previous reports, which can be attributed to the synergistic effect of the MB@ZIF-8/RGO nanocomposite with high surface area and excellent electro-conductivity.

### Selectivity studies

Considering the practical application of the prepared sensor, selectivity study was performed by introducing other species while the rutin concentration was fixed to 10  $\mu\text{M}$ . The limit of potential interfering substances was defined as  $\pm 5\%$  relative

**Table 1** Comparison of analytical performance of rutin at different modified electrodes

Modified materials	Methods	Linear ranges ( $\mu\text{M}$ )	Detection limits ( $\mu\text{M}$ )	Reference
IL-CPE <sup>a</sup>	CV	0.5–100.0	0.358	[28]
IL-CCE <sup>b</sup>	DPV	0.3–100.0	0.09	[29]
CeO <sub>2</sub> /GCE	DPV	0.5–500.0	0.2	[30]
SWCNTs <sup>c</sup> /CILE <sup>d</sup>	DPV	0.1–800.0	0.07	[31]
Nafion-GO <sup>e</sup> -IL/CILE	DPV	0.08–100.0	0.016	[32]
PtNPs <sup>f</sup> /RGO/GCE	DPV	0.057–102.59	0.02	[33]
PAMAM <sup>g</sup> /Graphene/GCE	DPV	0.001–2.0	0.0006	[34]
CCB <sup>h</sup> /Graphene/GCE	DPV	0.001–1000.0	0.00033	[35]
C-Ni/GCE	DPV	0.21–1.72	0.000602	[36]
MB <sup>i</sup> @ZIF-8 <sup>j</sup> /RGO/GCE	DPV	0.1–100.0	0.02	This work

<sup>a</sup> IL-CPE: ionic liquid modified carbon paste electrode; <sup>b</sup> IL-CCE: ionic liquid modified carbon ceramic electrode; <sup>c</sup> SWCNTs: single-walled carbon nanotubes; <sup>d</sup> CILE: carbon ionic liquid electrode; <sup>e</sup> GO: graphene oxide; <sup>f</sup> PtNPs: Pt nanoparticles; <sup>g</sup> PAMAM: poly(amidoamine) dendrimers; <sup>h</sup> CCB: conductive carbon black; <sup>i</sup> MB: methylene blue; <sup>j</sup> ZIF-8: Zeolitic imidazolate frameworks-8

error in the determination of rutin. It showed that 500 fold of  $K^+$ ,  $Na^+$ ,  $Mg^{2+}$ ,  $Ca^{2+}$ ,  $Cu^{2+}$ ,  $Fe^{3+}$ ; and 100-fold ratio of glucose, oxalic acid, glycine; 50-fold ratio of ascorbic acid, l-cysteine, and l-phenylalanine hardly influenced the accurate determination of rutin (signal change <5%) in Table S1 (in Electronic Supporting Material). Moreover, rutin often coexists with other flavonoids with similar structure. Therefore, the influence of some common flavonoids, quercetin, puerarin, apigenin, naringenin were also investigated (Fig. S5 in Electronic Supporting Material). The weak response currents for puerarin, apigenin and naringenin are investigated, indicating that these flavonoids cannot interfere the determination of rutin. For quercetin, although it has a significant electrochemical response in this case, its oxidation potential is distinguished from rutin. Such results indicated that the analytical method had good selectivity.

### Reproducibility and stability of the modified electrode

The reproducibility and stability of the MB@ZIF-8/RGO/GCE were investigated by the measurement of the response to the 100  $\mu$ M rutin. The relative standard deviation (RSD) of the oxidation peak current for 11 times successive measurements was calculate to be 1.6%. During the period of 21 days, the modified electrode was stored at 4 °C and intermittently measured the response current of 100  $\mu$ M rutin every 3 days. As a result, the peak currents remained about 96.7% of their initial values, reflecting the good stability of the modified electrode.

### Real sample determination

In order to examine the method in practical application, the compound rutin tablet samples were analyzed by using the experimental procedure. Prior to analysis, the tablets were ground into fine powder, and then accurately weighed and dissolved in ethanol to obtain a stock solution. Then the stock solution was diluted with 0.1 M phosphate buffer (pH 7.0) for analysis. Table S2 (in Electronic Supporting Material) shows the determination results with three parallel measurements and the recovery is calculated using the standard addition method. As can be seen, the recoveries of rutin are in the range of 96.33–103.50%, which indicates that the electrode is suitable for the detection of rutin in the drug samples. The proposed method was further applied to the biological samples urine to prove the practical applications. The results were shown in Table S3 (in Electronic Supporting Material). The samples were diluted with the buffer solution and the standard rutin solution was added to calculate the recovery. As can be seen, the recovery of rutin was in the range of 97.5–99.5%, which indicated that the proposed electrode was suitable for the detection of rutin in the biological samples.

## Conclusions

In summary, an electrochemical sensor based on MB@ZIF-8/RGO composite is successfully fabricated for the sensitive detection of rutin. The sensor exhibits excellent electrocatalytic for the sensitive detection of rutin due to the synergistic effects of MB and RGO (excellent electric conductivity and strong electrocatalytic) and large surface area of ZIF-8. The method has wide linear range, high sensitivity, good stability, and acceptable reproducibility. The modified electrode is further used to analyze rutin in tablet and urine samples with satisfactory results. These results indicate that the MB@ZIF-8/RGO sensor may have great potential applications in electrochemical sensing.

**Acknowledgements** We really appreciate the financial support from the National Natural Science Foundation of China (21645007 and 21475071), the Taishan Scholar Program of Shandong Province (no. ts201511027) and the Natural Science Foundation of Shandong (ZR2016BM21).

**Compliance with ethical standards** The authors declare that they have no competing interests.

## References

- Guo R, Wei P (2008) Studies on the antioxidant effect of rutin in the microenvironment of cationic micelles. *Microchim Acta* 161:233–239. <https://doi.org/10.1007/s00604-007-0888-7>
- Ishii K, Furuta T, Kasuya Y (2001) Determination of rutin in human plasma by high-performance liquid chromatography utilizing solid-phase extraction and ultraviolet detection. *J Chromatogr B* 759: 161–168
- Hassan HNA, Barsoum BN, Habib IHI (1999) Simultaneous spectrophotometric determination of rutin, quercetin and ascorbic acid in drugs using a Kalman filter approach. *J Pharm Biomed Anal* 20: 315–320. [https://doi.org/10.1016/S0731-7085\(99\)00048-5](https://doi.org/10.1016/S0731-7085(99)00048-5)
- Vinas P, Lopez-Erroz C, Marin-Hernandez JJ, Hernandez-Cordoba M (2000) Determination of phenols in wines by liquid chromatography with photodiode array and fluorescence detection. *J Chromatogr A* 871:85–93. [https://doi.org/10.1016/S0021-9673\(99\)01087-0](https://doi.org/10.1016/S0021-9673(99)01087-0)
- He C, Cui H, Zhao X, Zhao H, Zhao G (1999) Determination of Rutin by flow injection with inhibited Chemiluminescence detection. *Anal Lett* 32:2751–2759. <https://doi.org/10.1080/00032719908543003>
- Legnerova Z, Satinsky D, Solich P (2003) Using on-line solid phase extraction for simultaneous determination of ascorbic acid and rutin trihydrate by sequential injection analysis. *Anal Chim Acta* 497: 165–174. <https://doi.org/10.1016/j.aca.2003.07.007>
- Kang J, Lu X, Zeng H, Liu H, Lu B (2002) Investigation on the electrochemistry of rutin and its analytical application. *Anal Lett* 35:677–686. <https://doi.org/10.1081/AL-120003169>
- Zhou J, Zhang K, Liu J, Song G, Ye B (2012) A supersensitive sensor for rutin detection based on multi-walled carbon nanotubes and gold nanoparticles modified carbon paste electrodes. *Anal Methods* 4:1350–1356. <https://doi.org/10.1039/c2ay05930d>
- Wu Y, Hu CX, Huang M, Song N, Hu W (2015) Highly enhanced electrochemical responses of rutin by nanostructured Fe<sub>2</sub>O<sub>3</sub>/RGO

- composites. *Ionics* 21:1427–1434. <https://doi.org/10.1007/s11581-014-1310-1>
10. Li J, Sculley J, Zhou H (2011) Metal–organic frameworks for separations. *Chem Rev* 112:869–932
  11. Mason JA, Veenstra M, Long JR (2014) Evaluating metal–organic frameworks for natural gas storage. *Chem Sci* 5:32–51. <https://doi.org/10.1039/C3SC52633J>
  12. Wang C, Liu D, Lin W (2013) Metal-organic frameworks as a tunable platform for designing functional molecular materials. *J Am Chem Soc* 135:13222–13234. <https://doi.org/10.1021/ja308229p>
  13. Wang L, Han Y, Feng X, Zhou J, Qi P, Wang B (2016) Metal–organic frameworks for energy storage: batteries and supercapacitors. *Coord Chem Rev* 307:361–381. <https://doi.org/10.1016/j.ccr.2015.09.002>
  14. Kreno L, Leong K, Farha OK, Allendorf M, Duyne RVP, Hupp JT (2012) Metal–organic framework materials as chemical sensors. *Chem Soc Rev* 112:1105–1125
  15. Yu G, Xia J, Zhang F, Wang Z (2017) Hierarchical and hybrid RGO/ZIF-8 nanocomposite as electrochemical sensor for ultrasensitive determination of dopamine. *J Electroanal Chem* 801:496–502. <https://doi.org/10.1016/j.jelechem.2017.08.038>
  16. Xu J, Xia J, Zhang F, Wang Z (2017) An electrochemical sensor based on metal-organic framework-derived porous carbon with high degree of graphitization for electroanalysis of various substances. *Electrochim Acta* 251:71–80. <https://doi.org/10.1016/j.electacta.2017.08.114>
  17. Horcajada P, Chalati T, Serre C, Gillet B, Sebrie C, Baati T, Eubank JF, Heurtaux D, Clayette P, Kreuz C, Chang JS, Hwang YK, Marsaud V, Bories PN, Cynober L, Gil S, Férey G, Couvreur P, Gref R (2010) Porous metal–organic-framework nanoscale carriers as a potential platform for drug delivery and imaging. *Nature Mater* 9:172–178. <https://doi.org/10.1038/nmat2608>
  18. Shi LB, Zhua X, Liua TT, Zhao HL, Lan MB (2016) Encapsulating cu nanoparticles into metal-organic frameworks for nonenzymatic glucose sensing. *Sensors Actuators B* 227:583–559. <https://doi.org/10.1016/j.snb.2015.12.092>
  19. Xia J, Wang Z, Cai F, Zhang F, Yang M, Xiang W, Bi S, Gui R (2015) An electrochemical sensor for the sensitive detection of rutin based on a novel composite of activated silica gel and graphene. *RSC Adv* 5:39131–39137. <https://doi.org/10.1039/C5RA01338K>
  20. Xu J, Cao X, Xia J, Gong S, Wang Z, Lu L (2016) Phosphomolybdic acid functionalized graphene loading copper nanoparticles modified electrodes for non-enzymatic electrochemical sensing of glucose. *Anal Chim Acta* 934:44–51. <https://doi.org/10.1016/j.aca.2016.06.033>
  21. Xia J, Cao X, Wang Z, Yang M, Zhang F, Lu B, Li F, Xia L, Li Y, Xia Y (2016) Molecularly imprinted electrochemical biosensor based on chitosan/ionic liquid–graphene composites modified electrode for determination of bovine serum albumin. *Sens Actuators B Chem* 225:305–311. <https://doi.org/10.1016/j.snb.2015.11.060>
  22. Wang X, Wang Q, Wang Q, Gao F, Gao F, Yang Y, Guo H (2014) Highly dispersible and stable copper terephthalate metal–organic framework–graphene oxide nanocomposite for an electrochemical sensing application. *ACS Appl Mater Interfaces* 6:11573–11580. <https://doi.org/10.1021/am5019918>
  23. Zheng H, Zhang Y, Liu L, Wan W, Guo P, Nyström AM, Zou X (2016) One-pot synthesis of metal–organic frameworks with encapsulated target molecules and their applications for controlled drug delivery. *J Am Chem Soc* 138:962–968. <https://doi.org/10.1021/jacs.5b11720>
  24. Dong L, Chen M, Li J, Shi D, Dong W, Li X, Bai Y (2016) Metal-organic framework-graphene oxide composites: a facile method to highly improve the CO<sub>2</sub> separation performance of mixed matrix membranes. *J Membrane Sci* 520:801–811. <https://doi.org/10.1016/j.memsci.2016.08.043>
  25. Cravillon J, Münzer S, Lohmeier SJ, Feldhoff A, Huber K, Wiebcke M (2009) Rapid room-temperature synthesis and characterization of nanocrystals of a proto- typical zeolitic imidazolate framework. *Chem Mater* 21:1410–1412. <https://doi.org/10.1021/cm900166h>
  26. Laviron E (1979) General expression of the linear potential sweep voltammogram in the case of diffusionless electrochemical systems. *J Electroanal Chem Inter Electrochem* 101:19–28. [https://doi.org/10.1016/S0022-0728\(79\)80075-3](https://doi.org/10.1016/S0022-0728(79)80075-3)
  27. Yang S, Li G, Wang G, Zhao J, Qiao Z, Qu L (2015) Decoration of chemically reduced graphene oxide modified carbon paste electrode with yttrium hexacyanoferrate nanoparticles for nanomolar detection of rutin. *Sens Actuators B Chem* 206:126–132. <https://doi.org/10.1016/j.snb.2014.09.027>
  28. Sun W, Yang M, Li Y, Jiang Q, Liu S, Jiao K (2008) Electrochemical behavior and determination of rutin on a pyridinium-based ionic liquid modified carbon paste electrode. *J Pharmaceut Biomed* 48:1326–1331
  29. Zhan T, Sun X, Wang X, Hou W, Sun W (2010) Application of ionic liquid modified carbon ceramic electrode for the sensitive voltammetric detection of rutin. *Talanta* 82:1853–1857. <https://doi.org/10.1016/j.talanta.2010.07.083>
  30. Wei Y, Wang G, Li M, Wang C, Fang B (2007) Determination of rutin using a CeO<sub>2</sub> nanoparticle-modified electrode. *Microchim Acta* 158:269–274. <https://doi.org/10.1007/s00604-006-0716-5>
  31. Zhu Z, Sun X, Zhuang X, Zeng Y, Sun W, Huang X (2010) Single-walled carbon nanotubes modified carbon ionic liquid electrode for sensitive electrochemical detection of rutin. *Thin Solid Films* 519:928–933. <https://doi.org/10.1016/j.tsf.2010.09.013>
  32. Zeng B, Wei S, Xiao F, Zhao F (2006) Voltammetric behavior and determination of rutin at a single-walled carbon nanotubes modified gold electrode. *Sens Actuators B Chem* 115:240–246. <https://doi.org/10.1016/j.snb.2005.09.007>
  33. Li S, Yang B, Wang J, Bin D, Wang C, Zhang K, Du Y (2016) Nonenzymatic electrochemical detection of rutin on Pt nanoparticles/graphene nanocomposites modified glassy carbon electrode. *Chem Soc Rev* 8:5435–5440
  34. Yin H, Zhou Y, Cui L, Liu T, Ju P, Zhu L, Ai S (2011) Sensitive voltammetric determination of rutin in pharmaceuticals, human serum, and traditional Chinese medicines using a glassy carbon electrode coated with graphene nanosheets, chitosan, and a poly (amido amine) dendrimer. *Microchim Acta* 173:337–345. <https://doi.org/10.1007/s00604-011-0568-5>
  35. Lu L, Zhang F, Xia J, Wang Z, Liu X, Yuan Y (2015) Conductive carbon black-graphene composite for sensitive sensing of Rutin. *Int J Electrochem Sci* 10:1646–1657
  36. Duan L, Yang L, Xiong H, Zhang X, Wang S (2013) Studies on the electrochemistry of rutin and its interaction with bovine serum albumin using a glassy carbon electrode modified with carbon-coated nickel nanoparticles. *Microchim Acta* 180(5–6):355–361